Electronic Supplementary Material (ESI) for Journal of Materials Chemistry B

Supporting information: Gold Nanocages with Built-in Artificial Antibodies for Label-free Plasmonic Biosensing

Limei Tian†, Keng-Ku Liu†, Jeremiah J. Morrissey, Naveen Gandra, Evan D. Kharasch and Srikanth Singamaneni*

EM decay length calculation

In addition to bulk refractive index sensitivity, EM decay length is yet another important parameter to maximize a LSPR transducer response, which describes the distance-dependent refractive index sensitivity and sensing depth for LSPR sensors.[1-3] We employed layer-by-layer (LbL) assembly of polyelectrolytes for probing the distance-dependent LSPR sensitivity and EM decay length of AuNCs and AuNRs. LbL assembly of polyelectrolyte multilayers (PEM), which involves the alternate adsorption of oppositely charged polyelectrolytes, offers an excellent control over the thickness of the dielectric layer down to ~ 1nm.[4-9] The spectra revealed a progressive red-shift in LSPR wavelength and increase in LSPR intensity with the deposition of each bilayer due to the increase in the refractive index of the medium surrounding the plasmonic nanostructures (from air to polymer layer) (Fig. S4A and Fig. S4B). The cumulative LSPR wavelength shift following the deposition of each polyelectrolyte layer for AuNCs is much higher than AuNRs, especially within the first few nanometers where biomolecule binding events occur (Fig. S4D).

Owing to the evanescent nature of the EM field at the surface of the plasmonic nanostructures, the LSPR wavelength shift exhibits a characteristic decay with increasing distance from the surface of the nanostructures (*i.e.* increasing number of layers), given by [10, 11]

$$R = m\Delta\eta\left(1 - \exp\left(-2d/l\right)\right)$$

Where R is LSPR shift, m is the refractive index sensitivity of nanostructures, $\Delta\eta$ is the change in the refractive index in RIU, d is the adsorbate layer thickness (thickness of the polyelectrolyte layer in this case) and l is the EM decay length.

EXPERIMENTAL SECTION

Materials: Ethylene glycol (Lot. no K26B01) and sodium sulfide (Na_2S) were purchased from J. T. baker. Cetyltrimethylammonium bromide (CTAB), ascorbic acid, sodium borohydride, poly(styrene sulfonate) (PSS) (Mw=70,000 g/mol), and poly(allyl amine hydrochloride) (PAH) (Mw=56,000 g/mol), sodium borohydride ($NaBH_4$), Silver nitrate (purity higher than 99%), 4-aminothiophenol (pATP), glutaraldehyde (GA), poly(vinyl pyrrolidone) (PVP, Mw~29,000), chloroauric acid ($HAuCl_4$), myoglobin from human heart (Mw=17.7 kDa), hemopexin from human plasma (Mw=57 kDa), α_1-antitrypsin from human plasma (Mw=52 kDa), α_1-acid glycoprotein from human plasma (Mw=40.8 kDa), albumin from human serum (Mw=66.5 kDa), and hemoglobins human (Mw=64.5 kDa) were obtained from Sigma-Aldrich. Sucrose was purchased from G-Biosciences Inc. Poly(2-vinyl pyridine) (Mw=200,000 g/mol) was obtained from Scientific Polymer Products Inc. Artificial urine was purchased from Cerilliant Corp. Recombinant human fatty acid-binding protein 1 (FABP1)(MW=14.2 kDa), and recombinant human fatty acid binding protein-3 (FABP3)(MW=14.8 kDa) were obtained from RayBiotech, Inc. Recombinant neutrophil gelatinase associated lipocalin was obtained from SunnyLab (Kent, United Kingdom). All the chemicals have been used as received with no further purification.

Synthesis of silver nanocubes and gold nanocages (AuNCs): Prior to synthesis, all the glassware was cleaned using aqua regia (3:1 volume ratio of 37% hydrochloric acid and concentrated nitric acid). Silver nanocubes were synthesized using a sulfide-mediated method developed by Xia group.[12] Briefly, 90 µl of Na_2S solution (3 mM) in ethylene glycol was added to 6 ml of preheated ethylene glycol at 160 ºC in a disposable glass vial. After 8 min, 1.5 ml of PVP (0.02 g/ml) in ethylene glycol was added to the above mixture, immediately followed by the addition of 0.5 ml of $AgNO_3$ (0.048 g/ml) in ethylene glycol. The reaction was complete in 10 min with a dark ruddy-red meniscus in reaction solution. The product was washed with acetone and water by centrifugation. 10ml of aqueous PVP solution (9 mM) was add to 1 ml of the above mentioned silver nanocubes solution. After bringing the suspension to a mild boil for approximately 10 min, 1 mM $HAuCl_4$ was injected at a rate of 0.5 ml/min under vigorous stirring until dark

blue color appeared. The product was centrifuged once and redispersed in nanopure water before using (18.2 MΩ-cm).

Synthesis of gold nanorods: Gold nanorods were synthesized using a seed-mediated approach. [13, 14] Seed solution was prepared by adding 0.6 mL of an ice-cold solution of 10 mM sodium borohydride into 10 mL of vigorously stirred 0.1 M CTAB and 2.5×10^{-4} M $HAuCl_4$ aqueous solution at room temperature. The color of the seed solution changed from yellow to brown. Growth solution was prepared by mixing 95 mL of 0.1 M CTAB, 1.0 mL of 10 mM silver nitrate, 5 mL of 10 mM $HAuCl_4$, and 0.55 mL of 0.1 M ascorbic acid in the same order. The solution was homogenized by gentle stirring. To the resulting colorless solution, 0.12 mL of freshly prepared seed solution was added and set aside in dark for 14 h. Prior to use, the AuNRs solution was centrifuged at 13,000 rpm for 10 min to remove excess CTAB and redispersed in nanopure water.

Adsorption of AuNR on glass surface: To adsorb gold nanocages onto glass substrates, the glass substrates were coated with poly(2-vinyl pyridine) (P2VP) by exposing the piranha cleaned substrates to 1% (w/v) P2VP solution in ethanol.[15, 16] After rinsing the substrate with ethanol and drying with a stream of nitrogen, it was exposed to AuNCs solution for overnight to enable adsorption of the gold nanocages. Finally, the substrate was rinsed with water to remove the loosely bound nanocages, leaving a highly dense layer of nanocages on the surface.

Molecular Imprinting Procedure: Firstly, AuNC adsorbed glass substrate was placed in 2 ml of 100 mM $NaBH_4$ aqueous solution for 5 minutes with gentle shaking to remove PVP coating from AuNCs surface, followed by thorough rinsing with nanopure water.[17] Subsequently, AuNCs adsorbed on the substrate were modified with p-ATP and glutaraldehyde as crosslinkers by immersing the substrate in 2 ml of phosphate borate buffer (pH 8.3) containing 4 µl of glutaraldehyde (25%) and 4 µl of pATP (4mM in ethanol) for 1 minute, followed by rinsing with pH 8.3 buffer. In the next step, template protein (NGAL) was immobilized on nanocages by exposing the substrate to 115 µg/ml of NGAL in pH 8.3 buffer solution at 4°C for 2.5 hours, followed by rinsing with pH 8.3 buffer solution. Subsequently, the NGAL-coated substrate was immersed in 3ml of phosphate buffered saline (PBS, pH 7.5) containing 15 µl of TMPS and 15 µl of APTMS

for 40 minutes. Then the substrate was rinsed with buffer solution and stored in PBS solution at 4°C overnight. Finally, proteins were released by shaking the substrate in 2 ml of oxalic acid (10 mM) in 2% aqueous sodium dodecyl sulfate (SDS) solution.

NGAL detection and interfering proteins test: After removing template proteins, the molecularly imprinted AuNCs on glass substrates were immersed in 1 ml of different concentrations of NGAL in pH 8.3 buffer solution, followed by gently shaking for 30 minutes and then incubation at 4°C for 3.5 hours. The same procedure was used to test interfering proteins, including myoglobin from human heart(10 μg/ml), hemopexin from human plasma(10 μg/ml), antitrypsin from human plasma(10 μg/ml), acid glycoprotein from human plasma(10 μg/ml), albumin from human serum(10 μg/ml), hemoglobin(10 μg/ml), FABP1(1 μg/ml) and FABP3(1 μg/ml). Extinction spectra were collected from at least three samples for different concentrations of NGAL and interfering proteins to obtain the average LSPR wavelength shift.

*NGAL in different pH value and specific gravity of artificial urine test***:** The molecularly imprinted AuNCs coated substrates were immersed in 1 ml of 230 ng/ml NGAL in artificial urine with different pH (4.5, 5.5, 6.5, 7.5 and 8.5) and specific gravity (1.005, 1.010, 1.020, 1.030), followed by gently shaking for 30 minutes and incubation at 4°C for 3.5 hours. Extinction spectra were collected from at least three samples to obtain average LSPR wavelength shift.

Characterization: Transmission electron microscopy (TEM) micrographs were recorded on a JEM-2100F (JEOL) field emission instrument. Samples were prepared by drying a drop of the solution on a carbon-coated grid, which had been previously made hydrophilic by glow discharge. Scanning electron microscope (SEM) images were obtained using a FEI Nova 2300 Field Emission SEM at an accelerating voltage of 10 kV. Shimadzu UV-1800 spectrophotometer was employed for collecting UV-vis extinction spectra from solution and substrates.

A

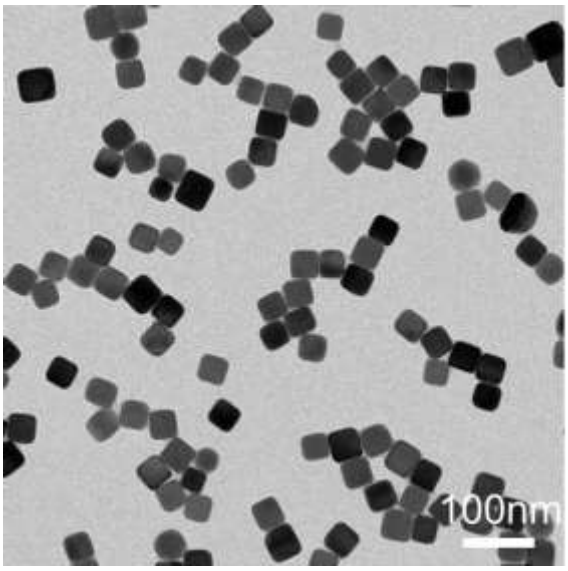

Figure S1: TEM image of silver nanocubes as template for gold nanocages.

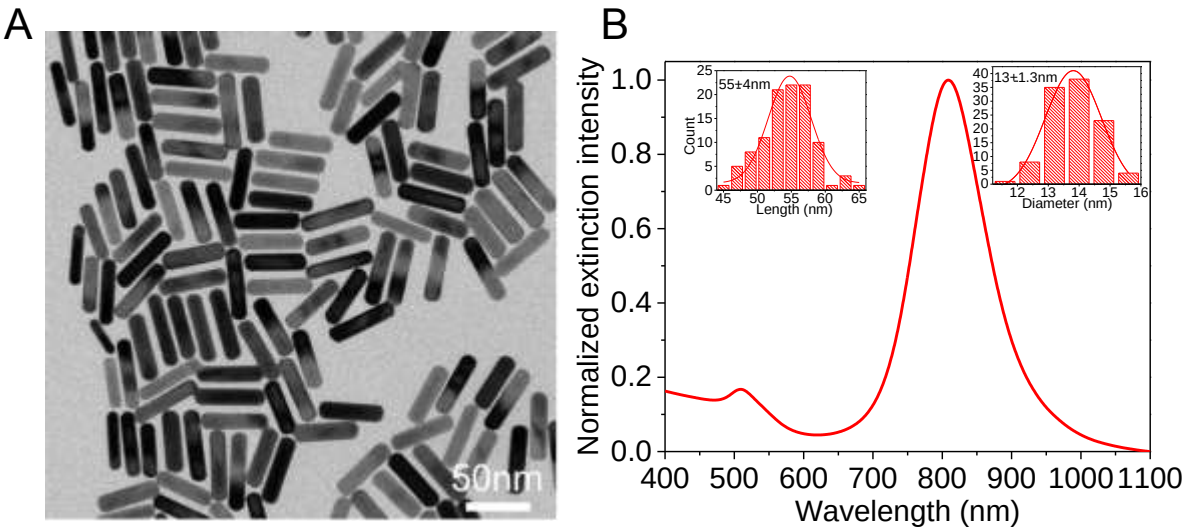

Figure S2: (A) TEM image of Au nanorods. (B) Vis-NIR extinction spectrum of the aqueous suspensions of Au nanorods (inset shows the histogram of the size distribution as measured from TEM images).

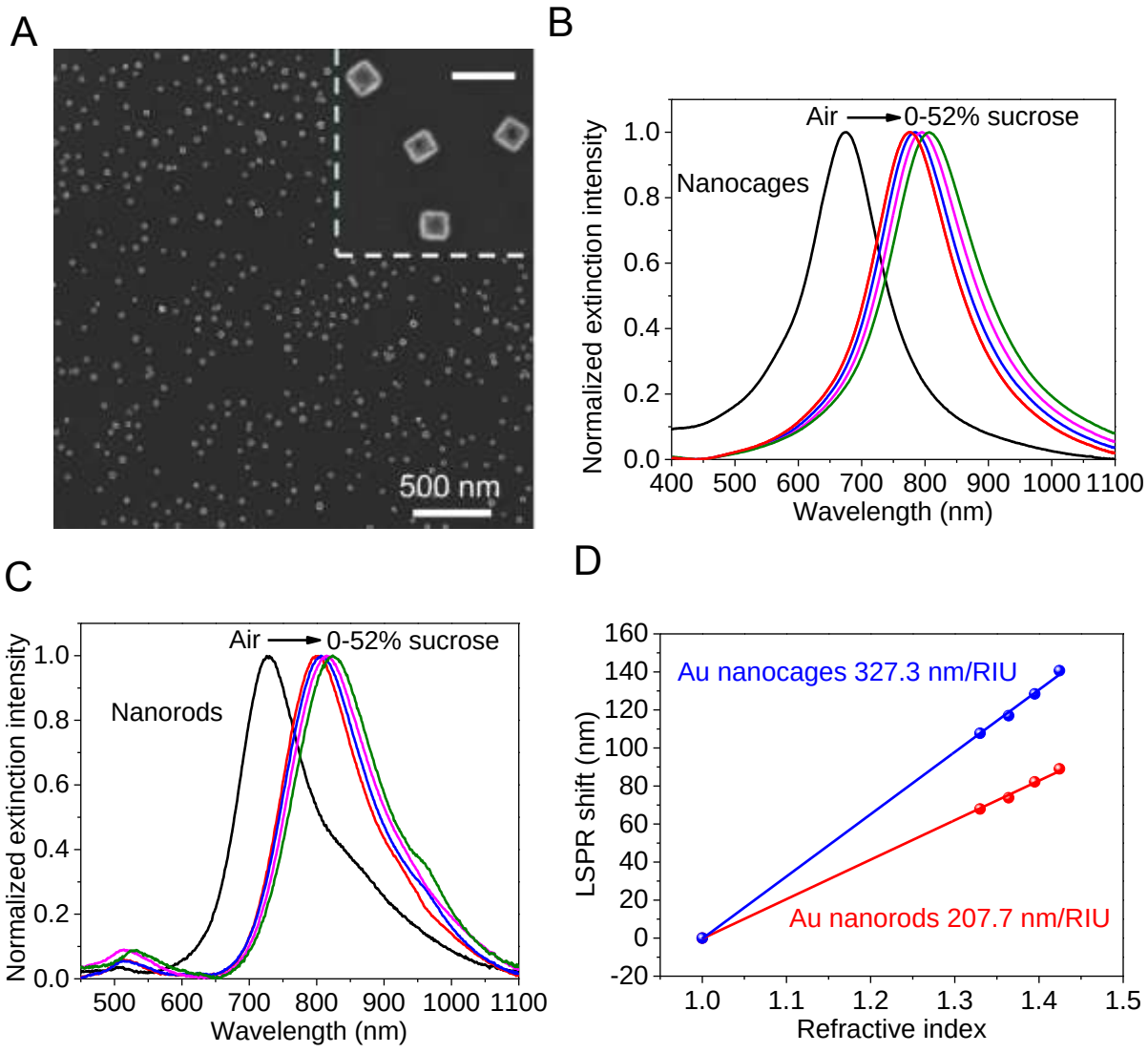

Figure S3: (A) SEM of Au nanocages adsorbed on a glass substrate. Vis-NIR extinction spectra of (B) Au nanocages and (C) Au nanorods in air and different concentrations of sucrose aqueous solution. (D) Comparison of bulk refractive index sensitivity of Au nanocages and nanorods.

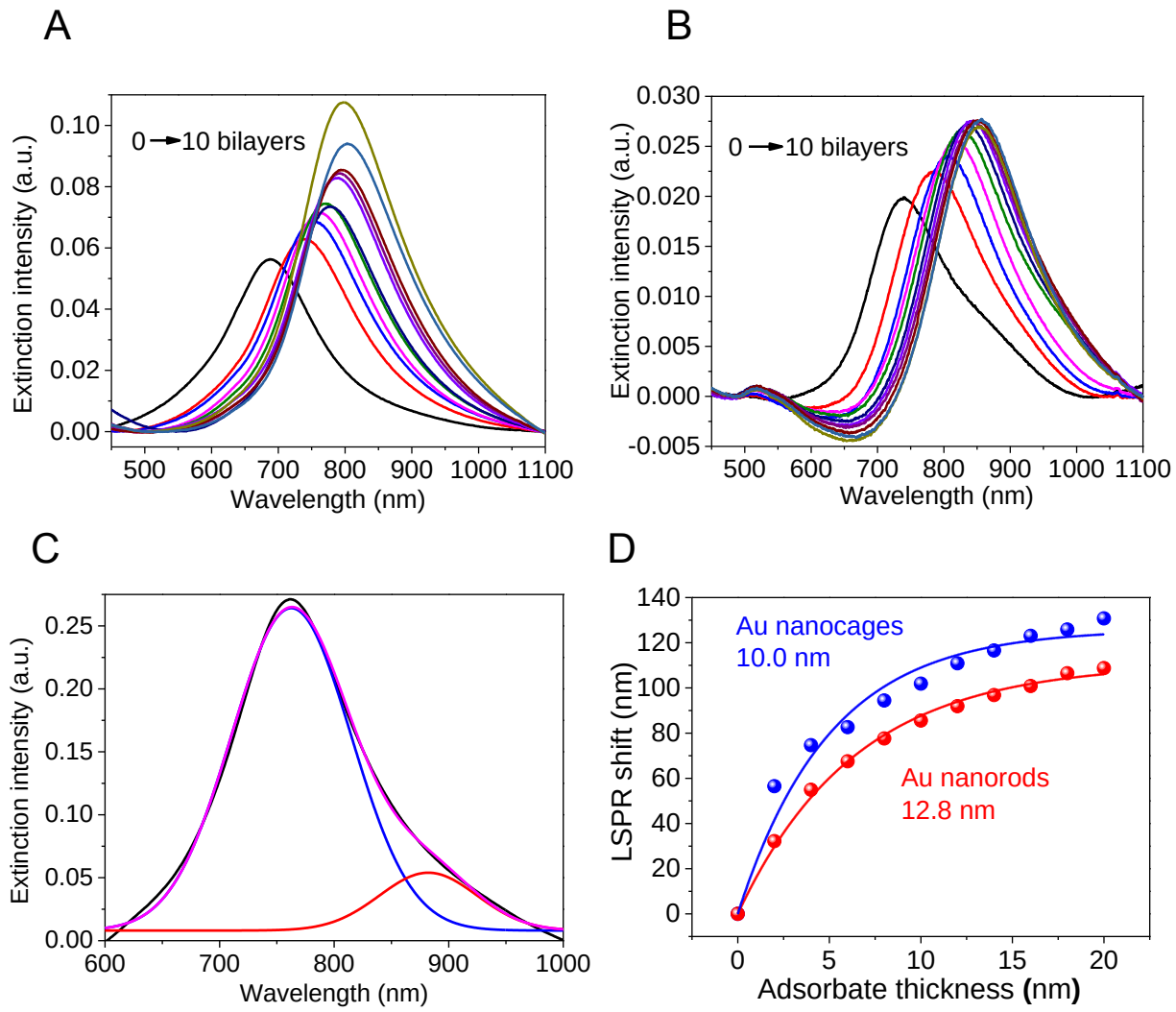

Figure S4: Vis-NIR extinction spectra of (A) AuNCs and (B) AuNRs following the deposition each polyelectrolyte bilayer showing a progressive red-shift and increase in the intensity of the longitudinal plasmon band. (C) Representative LSPR spectrum of AuNCs deconvoluted using two Gaussian peaks. (D) Comparison of distance dependent refractive index sensitivity of Au nanocages and nanorods.

References

1. A. J. Haes, S. Zou, G. C. Schatz and R. P. Van Duyne, *J. Phys. Chem. B*, 2004, **108**, 6961-6968.
2. A. J. Haes, S. Zou, G. C. Schatz and R. P. Van Duyne, *J. Phys. Chem. B*, 2003, **108**, 109-116.
3. A. V. Whitney, J. W. Elam, S. Zou, A. V. Zinovev, P. C. Stair, G. C. Schatz and R. P. Van Duyne, *J. Phys. Chem. B*, 2005, **109**, 20522-20528.
4. O. Kedem, A. B. Tesler, A. Vaskevich and I. Rubinstein, *ACS Nano*, 2011, **5**, 748-760.
5. G. Decher, *Science*, 1997, **277**, 1232-1237.
6. J. Park, L. D. Fouche and P. T. Hammond, *Adv Mater*, 2005, **17**, 2575-+.

7. A. A. Antipov, G. B. Sukhorukov and H. Mohwald, *Langmuir*, 2003, **19**, 2444-2448.
8. E. Kharlampieva, V. Kozlovskaya, J. Chan, J. F. Ankner and V. V. Tsukruk, *Langmuir*, 2009, **25**, 14017-14024.
9. L. M. Tian, M. Fei, R. Kattumenu, A. Abbas and S. Singamaneni, *Nanotechnology*, 2012, **23**.
10. J. N. Anker, W. P. Hall, O. Lyandres, N. C. Shah, J. Zhao and R. P. Van Duyne, *Nat Mater*, 2008, **7**, 442-453.
11. G. J. Nusz, A. C. Curry, S. M. Marinakos, A. Wax and A. Chilkoti, *ACS Nano*, 2009, **3**, 795-806.
12. S. E. Skrabalak, L. Au, X. D. Li and Y. N. Xia, *Nat. Protoc.*, 2007, **2**, 2182-2190.
13. B. Nikoobakht and M. A. El-Sayed, *Chem. Mater.*, 2003, **15**, 1957-1962.
14. C. J. Orendorff and C. J. Murphy, *J. Phys. Chem. B*, 2006, **110**, 3990-3994.
15. S. Malynych, I. Luzinov and G. Chumanov, *J. Phys. Chem. B*, 2002, **106**, 1280-1285.
16. L. M. Tian, E. Chen, N. Gandra, A. Abbas and S. Singamaneni, *Langmuir*, 2012, **28**, 17435-17442.
17. S. M. Ansar, F. S. Ameer, W. Hu, S. Zou, C. U. Pittman and D. Zhang, *Nano Lett.*, 2013, **13**, 1226-1229.